Aust. J. Phys., 1984, **37**, 75–90

A Theoretical Study of an Airborne Laser Technique for determining Sea Water Turbidity

D. M. Phillips and B. W. Koerber

Electronics Research Laboratory, Defence Research Centre Salisbury, Department of Defence, G.P.O. Box 2151, Adelaide, S.A. 5001.

Abstract

An airborne laser technique for remote measurement of sea water turbidity is studied theoretically. The limits of validity of an analytic model are established using Monte Carlo simulation computations. It is shown that, if the field of view of the airborne receiver is large enough, the backscatter signal from the water is attenuated at a rate determined by the absorption coefficient of the water. Apart from geometrical factors, the amplitude of the backscatter signal at the water surface depends on the scattering coefficient of the water. The method therefore allows both the absorption and scattering coefficients of water to be determined independently.

1. Introduction

The need for faster and more efficient techniques for charting coastal waters has led to the development of airborne laser systems for determining water depth. Several experimental systems have been built in the U.S.A. The feasibility of the technique was first demonstrated with a system constructed at the Syracuse University Research Corporation (Hickman and Hogg 1969). More extensive laboratory and airborne experiments with a system developed by the National Aeronautics and Space Administration were described by Kim (1977). Performance results of the more recent NASA Airborne Oceanographic Lidar (AOL) system, which has a higher data recording rate and a scanning capability, are described by Hoge *et al.* (1980).

In Australia, investigations into laser depth sounding techniques commenced at the Defence Research Centre Salisbury (DRCS) in response to a request in 1972 from the Royal Australian Navy (Calder 1980). An experimental Laser Airborne Depth Sounder (WRELADS I) was built and tested in 1976 and 1977. The operation of the system and some preliminary results obtained by it were described by Clegg and Penny (1978). Another system (WRELADS II) having full scanning, data recording, and horizontal position fixing capabilities has been developed and is undergoing flight trials (Penny 1982).

The primary limit on the performance of all laser depth sounding systems is the turbidity of the water through which the laser beam must pass. Some studies of the dependence of the maximum measurable depth on water turbidity have been carried out; for example, Hickman and Hogg (1969) performed several laboratory measurements, and other water turbidity measurements have been made from boats in conjunction with aircraft trials, but published data are scant.

0004-9506/84/010075$02.00

The paucity of such data may be due to the fact that boat work is both slow and susceptible to adverse weather conditions, making it difficult to coordinate with aircraft trials. The depth sounding performance of laser systems would therefore be much easier to evaluate if reliable airborne techniques for determining water turbidity could be developed. Moreover, surveys of water turbidity, such as that of the waters of Gulf St Vincent in South Australia reported by Phillips and Scholz (1982), would become easier and faster.

Ivanov *et al.* (1972) reported an experimental study of the relationship between water turbidity and the decay of the backscatter signal produced when a laser pulse propagates through water. They provided evidence that, with the geometry of their optical system, the attenuation coefficient of the backscatter signal initially approximates the beam attenuation coefficient c, but approaches the absorption coefficient a at greater depths. Similar experiments by Sizgoric and Carswell (1973) failed to find the agreement expected between the backscatter attenuation coefficient and c.

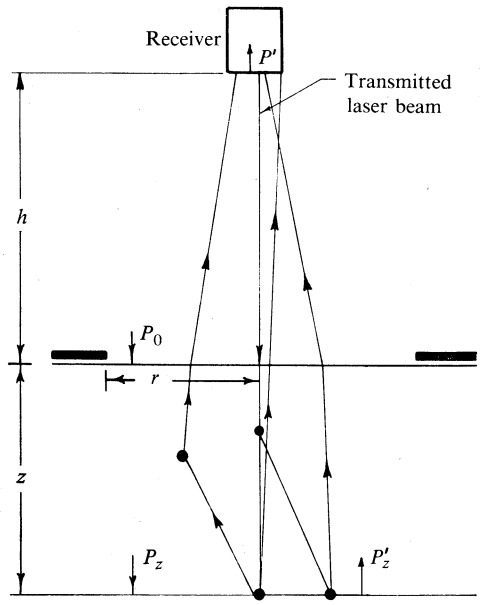

Fig. 1. Schematic diagram for the theoretical model of laser backscatter from water.

A recent paper by Gordon (1982) presented the results of a simulation study of the backscattering of laser pulses in water using a semi-analytic Monte Carlo method. He concluded that the attenuation coefficient of the backscatter signal lies between c and the diffuse attenuation coefficient K, depending on the field of view of the receiver optics.

The present paper presents a theoretical study of light backscattered from a laser pulse propagating in water ranging from clear to very turbid. Both analytic and Monte Carlo techniques are used to examine the parameters which govern the amplitude and attenuation of the backscatter signal. The dependence of the effective attenuation coefficient in the simple analytic model on water turbidity and receiver field of view is investigated. Also, the semi-analytic and full Monte Carlo methods are compared.

2. Theoretical Model of Laser Backscatter from Water

A schematic diagram illustrating the theoretical model is given in Fig. 1. An aircraft at height h transmits a laser pulse downwards to the water, in which it is partially absorbed and scattered. Some of the backscattered light travels upwards until it is collected again in a receiver. The diagram illustrates some of the singly and multiply scattered rays likely to be present.

(*a*) *Assumptions*

The laser pulse is assumed to be instantaneous, to have negligible diameter, and to be transmitted vertically downwards towards the water surface. These assumptions have no significant influence on the results obtained using this model.

A flat horizontal water surface is assumed. This could influence the results because waves could change the amount of backscattered light detected by the receiver. A calculation of the influence of surface waves on the results could be developed by extending the theoretical model described by Phillips (1979) to the transmission case.

The water is assumed to be homogeneous and isotropic: there is no reason to doubt that the water is isotropic and the observations by Phillips and Scholz (1982) indicate that vertical homogeneity of the water column is a valid assumption under some conditions. The turbidity of the water is one of the main variables in this model.

The receiver is assumed to be concentric with the transmitter and to have a small diameter and a variable field of view. In practice the receiver is located next to the transmitter, but this difference is negligible in theoretical terms. The variable field of view is represented in the model as an aperture of radius r at the water surface, as shown in Fig. 1.

(*b*) *Theoretical Model*

When the laser emits a pulse of energy Q, the radiant flux incident on the water surface is

$$P_0(t) = Q\,\delta(t), \tag{1}$$

where $\delta(t)$ is the Dirac delta function, so that

$$\int P_0(t)\,\mathrm{d}t = Q. \tag{2}$$

The radiant flux reaching a plane at depth z is given approximately by

$$P_z(t) = (1-\rho)\exp(-kz)\,P_0(t - z/v), \tag{3}$$

where ρ is the reflection coefficient of the water surface, k is the effective attenuation coefficient for the laser light, and v is the speed of light in water. Two approximations are involved in this equation. Firstly, the radiant flux at a given depth is no longer a precise delta function, because the scattered light travels further than the unscattered light and is delayed in time. Secondly, k is not strictly a constant; its value will change as the laser light becomes less directional and more diffuse. Both approximations can be expected to fail when the average number of scattering collisions becomes large.

The radiant flux $P'_z(t)$ scattered upwards from the plane at depth z and at time t, within the solid angle subtended by the receiver, is approximately given by

$$P'_z(t) = \{\beta(\pi)A/h^2n^2\} \int_0^\infty \exp(-kv\tau)\, P_{z+v\tau}(t-\tau)\, \tfrac{1}{2}v\, \mathrm{d}\tau, \tag{4}$$

where A is the area of the receiver aperture, n is the refractive index of the water, and $\beta(\pi)$ is the value of the volume scattering function $\beta(\theta)$ when $\theta = \pi$. In this equation the depth z has been neglected compared with the aircraft height h. Evaluation of the integral, using equations (2) and (3), yields

$$P'_z(t) = (A/2h^2n^2)(1-\rho)v\,\beta(\pi)\exp(-kz)Q, \tag{5}$$

when $t = z/v$. Provided that the angular field of view of the receiver is large enough to include essentially all the backscattered light directed towards the receiver, the radiant flux reaching the receiver is therefore given by

$$P'(t) = (A/2h^2n^2)(1-\rho)^2 v\,\beta(\pi)\exp(-2kvt)Q. \tag{6}$$

This equation is analogous to Gordon's (1982) equation (1) when the substitution $Q = P_0\, \mathrm{d}t$ is made.

It is clear from the derivation that this result depends on two important assumptions. Firstly, the number of scattering collisions must remain small so that the laser light remains strongly directional. Secondly, the angular field of view of the receiver must be sufficiently large.

(c) *Effective Attenuation Coefficient*

In obtaining equation (6), no assumption was made about the magnitude of the effective attenuation coefficient k. Since it describes the effect of water turbidity on the signal, it is related in some way to the intrinsic optical properties of the water, namely a, the volume absorption coefficient; b, the volume total scattering coefficient; and c, the volume attenuation coefficient*; where

$$a+b = c. \tag{7}$$

These coefficients are macroscopic phenomenological parameters and are defined within the context of radiative transfer theory for a small volume in the limit of that volume approaching zero. Preisendorfer (1977) derived operational definitions of these parameters in terms of measurable radiometric quantities at a point:

$$a = -\nabla . \boldsymbol{H}/h, \tag{8}$$

$$b = h_*/h, \tag{9}$$

$$c = (N_* - \mathrm{d}N/\mathrm{d}r)/N, \tag{10}$$

where N is the radiance, h and $\boldsymbol{H}$ are the scalar and vector irradiances respectively, and h_* is the integral of the path function N_* over all solid angles, at the point concerned.

* This is the nomenclature adopted by the International Association for Physical Sciences of the Ocean (see Tyler 1977, p. 42).

Defined in this way, these intrinsic optical parameters represent an ensemble average over the particles actually present. In the zero volume limit, these properties may be considered as describing a 'representative' single particle. In the Monte Carlo calculations described in the next section, each photon is traced through a series of single scattering interactions with such 'representative' particles. This procedure is used in other Monte Carlo studies of light scattering, both in clouds (see e.g. Plass and Kattawar 1971; Platt 1981) and in water (see e.g. Poole *et al.* 1981; Gordon 1982).

The measurement of the intrinsic optical properties of water defined above requires the realization of the operational definitions in experimental equipment. The design considerations involved in the measurement of absorption were described by Gilbert *et al.* (1969) and those related to the measurement of attenuation were discussed by Austin and Petzold (1977). The experimental data reported in Section 3*b* were obtained using instruments designed on these principles. Thus, although the accuracy of the data is limited by multiple scattering effects, the quantities measured were single scattering properties of the 'representative' particles used in the Monte Carlo calculations.

(*d*) *Large Field of View Limit*

When the field of view of the receiver is large enough, all photons emerging from the water within the solid angle subtended by the receiver are detected. In this case, some limits on the magnitude of the effective attenuation coefficient k can be postulated.

In the derivation of equation (6), k is assumed to be independent of depth. However, because the angular distribution of the light changes with depth, the value of k will also change with depth and use must be made of the diffuse attenuation function for irradiances

$$K(z, \pm) \equiv -H(z, \pm)^{-1}\, \mathrm{d}H(z, \pm)/\mathrm{d}z, \tag{11}$$

where $H(z, \pm)$ are the downwelling $(-)$ and *detected* upwelling $(+)$ irradiances at depth z. For the upwelling light to reach the detector it must be (almost) collimated at the water surface, similar to the downward beam. Thus the upward photon paths are reciprocals of downward paths and the distinction between upwelling and downwelling parameters becomes superfluous.

The changing angular distribution of light with depth can be taken into account in equation (6) by making the replacement

$$kvt = \int_0^{vt} K(z)\, \mathrm{d}z, \tag{12}$$

where $K(z) = K(z, +) = K(z, -)$. The general expression for the diffuse attenuation function given by Preisendorfer (1977) reduces in the present context to

$$K(z) = [a + b_\mathrm{b}\{1 - \varepsilon(z)\}]D(z), \tag{13}$$

where $\varepsilon(z)$ is a somewhat complicated but small term. The backscattering coefficient b_b is defined in terms of the volume scattering function $\beta(\theta)$ by

$$b_\mathrm{b} = 2\pi \int_{\frac{1}{2}\pi}^{\pi} \beta(\theta) \sin\theta\, \mathrm{d}\theta. \tag{14}$$

The angular distribution function

$$D(z) = \int N \, d\Omega \Big/ \int N \cos\theta \, d\Omega \geqslant 1 \tag{15}$$

is unity for a vertical collimated beam and increases as the light becomes more diffuse. From equations (12)–(15) it can be shown that k must satisfy the inequality

$$a < k < (a+b_b)D(vt). \tag{16}$$

The lower limit corresponds to the near-surface case in relatively clear water when the light is collimated [$D(z) \approx 1$] and backscattering losses are negligible ($b_b \ll a$). The latter is true if the 'albedo for single scattering', defined as

$$\omega_0 = b/c, \tag{17}$$

is small, since the ratio b/a is then small and b_b/a is much smaller. The upper limit in (16) describes the deep water case in turbid water when the light is diffuse and backscattering losses are significant.

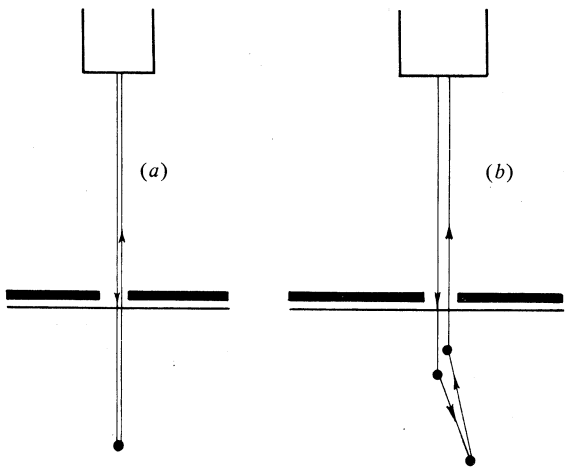

Fig. 2. Schematic diagram of the small field of view limit for laser backscatter from water for (*a*) singly and (*b*) multiply scattered components.

(*e*) *Small Field of View Limit*

As the field of view of the receiver is reduced the coefficient k in equation (6) departs further and further from the range given by (16). When the field of view is very small the received signal contains two components, as illustrated in Fig. 2. The first component (Fig. 2*a*) is the light which suffers no scattering collisions, apart from the single backscattering collision that directs the light upwards again. Since this component excludes all multiply scattered light k corresponds to the beam attenuation coefficient c.

However, the received signal also includes a multiply scattered component (Fig. 2*b*). In this case the downward light is scattered one or more times out of the original direction; it is then backscattered and scattered a further time into a vertical direction. This multiply scattered component adds to the signal received and thereby reduces k below the value of c.

In the small field of view limit, the effective attenuation coefficient k is expected to approach c when ω_0 is small. The probability of multiple scattering is then small. On the other hand, when ω_0 is large (e.g. approaching unity) multiple scattering will contribute and k will be less than c.

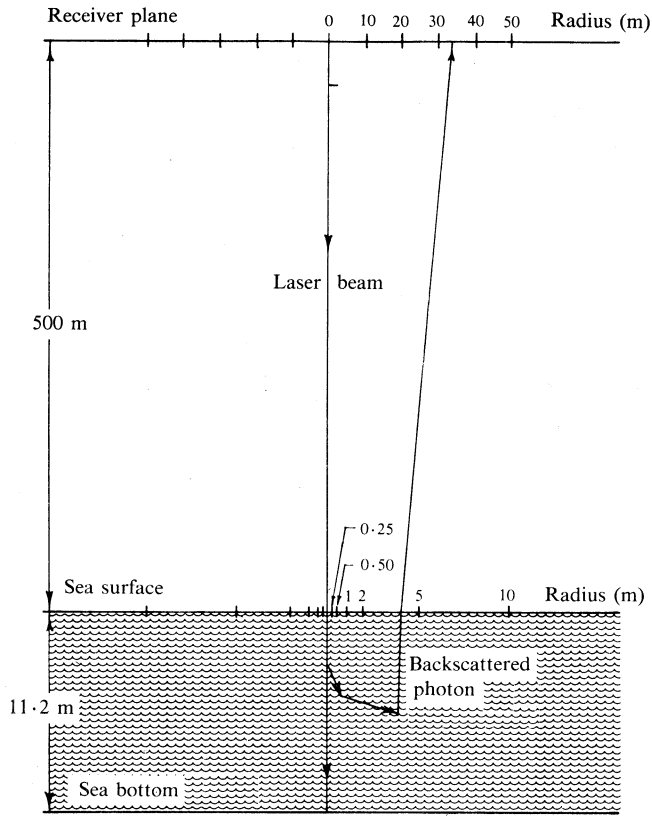

Fig. 3. Geometry used for the Monte Carlo simulation model.

3. Monte Carlo Simulation of Laser Backscatter from Water

The dependence of k on the receiver field of view and on the albedo for single scattering was investigated in a Monte Carlo simulation. The simulation model was established with a set of assumptions corresponding to those used in the analytic model discussed in Section 2*a*: a laser impulse of infinitesimal diameter was assumed to be transmitted vertically downwards towards a flat sea surface; the geometry used for the model is shown in Fig. 3.

(*a*) *Description of the Monte Carlo Model*

The model simulates the random passage in water of individual photons from the transmitted light beam through a series of scatterings until the photons reach the upper and lower boundaries of the sea water medium or move laterally well outside the field of view of the airborne optical receiver. For each segment of a photon trajectory, values are determined for the distance travelled before scattering and for

the scattering angles by making random selections from cumulative probability data for these parameters. Random numbers required for this procedure are generated using the multiplicative congruential method in a subroutine of the program. Weighting factors are computed for each photon trajectory to account for the absorption losses along that path. Transit times through the water are computed for each photon path. After the computations have been repeated for a large number of photons, a space–time map is built up of the distribution of light flux in the water.

For each photon that is backscattered from sea water, tests are carried out in the program to determine whether this photon is within the field of view and travelling towards the entrance aperture of the airborne receiver. Allowance is made for a change in direction at the sea surface due to refraction at this interface. Totals are kept of the numbers of photons (weighted for the effects of absorption) collected at the receiver during successive 5 ns intervals of photon travel time. To examine the effect of changing the field of view of the receiver, sub-totals are kept of the numbers of these photons collected from concentric annular regions at the sea surface having radii 0·25, 0·50, 1·0, 2·0, 5·0 and 10·0 m.

Very large numbers of photon trajectories were computed to reduce the chance variations produced in the results due to the random Monte Carlo process used in this simulation study. In order to keep computing times within manageable limits, it was decided to substantially increase the effective collecting area of the optical receiver in the model, thereby producing considerable smoothing of results by averaging over the much larger area. Hence in the model, the photons are counted as they arrive in the concentric annular regions in the receiver aperture plane having radii 10, 20, 30, 40 and 50 m. Totals obtained for these larger areas can be scaled to provide results relevant to the actual receiver size (180 mm diameter).

The computer program is executed in a series of separate runs and after each run the output data are combined in a single data set. As each additional run is carried out, an assessment is made of the magnitude of the random errors in the data due to the Monte Carlo process. These errors are progressively reduced as the data sample size is increased. The computations are continued until the random errors are reduced to an acceptable level.

A more efficient semi-analytic Monte Carlo procedure was also used in some cases for comparison. This method uses statistical weights in a similar way to that reported by Plass and Kattawar (1971) and Platt (1981) for cloud studies and by Poole *et al.* (1981) and Gordon (1982) for oceanic lidar studies. At each photon collision, the probability that the photon will scatter in such a direction so that it reaches the detector *without further collisions* is calculated. This semi-analytic method typically achieves the same statistical accuracy as the *full* Monte Carlo method with a reduction in computing time of several orders of magnitude.

(b) Data on Optical Properties of Water

The computations were carried out for the full range of turbidities reported in the survey by Phillips and Scholz (1982), as well as for more turbid conditions, so that the limits of validity of the analytic model could be explored. The values of the beam attenuation coefficient c chosen were 0·1, 0·5, 2·0 and 5·0 m^{-1}.

The contributions of absorption and scattering to these levels of attenuation were determined from an experimental study of the relationship between absorption and attenuation coefficients. The absorption coefficient was determined using the absorp-

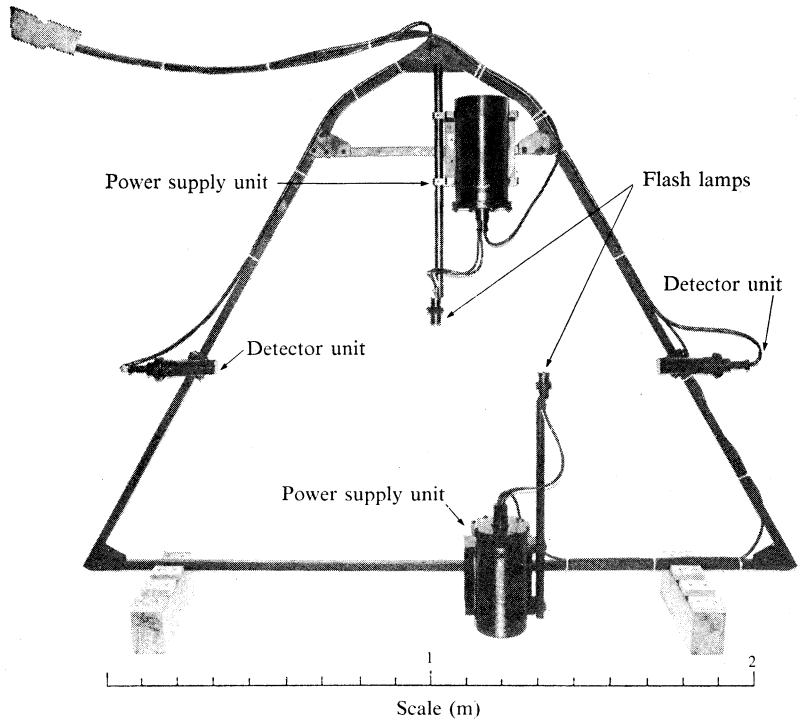

Fig. 4. The DRCS absorption meter.

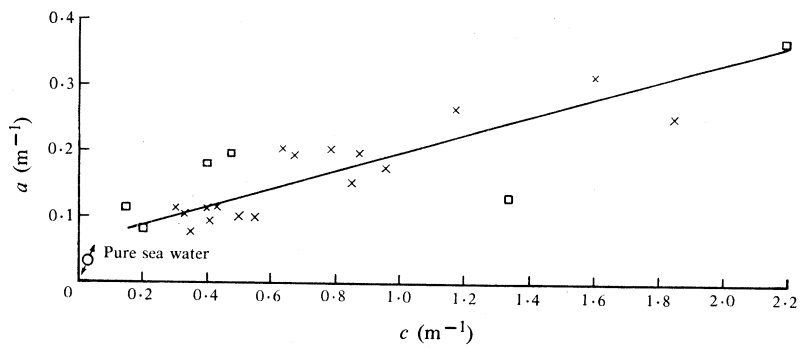

Fig. 5. Comparison of the measured values of absorption and beam attenuation coefficients a and c at a wavelength of 530 nm: crosses, the present DRCS data; squares, the Scripps data of Petzold (1972). The regression line $a = 0{\cdot}0586 + 0{\cdot}139c$ has been fitted to the DRCS data.

tion meter shown in Fig. 4, which was made at DRCS to the design described by Gilbert *et al.* (1969) and produced at the Stanford Research Institute (see also Bauer *et al.* 1971). The beam attenuation coefficient c was determined using a transmissometer designed and made at DRCS (see Phillips and Scholz 1982), using a concept described by Austin and Petzold (1977). The measurements were made at numerous locations in Gulf St Vincent, South Australia, in order to cover an adequate range of turbidities.

The results are presented in Fig. 5 where, for comparison, several examples of data (squares) measured at the Scripps Institution of Oceanography by Petzold (1972) are also included. There is general agreement between the two sets of data, but the values of the absorption coefficient a determined by Petzold are somewhat higher in relatively clear water than those determined in the DRCS study.

For the Monte Carlo simulation, a regression line was fitted to the DRCS data and used to determine the value of a corresponding to each value of c. The values of the scattering coefficient b were derived from the defining equation (7).

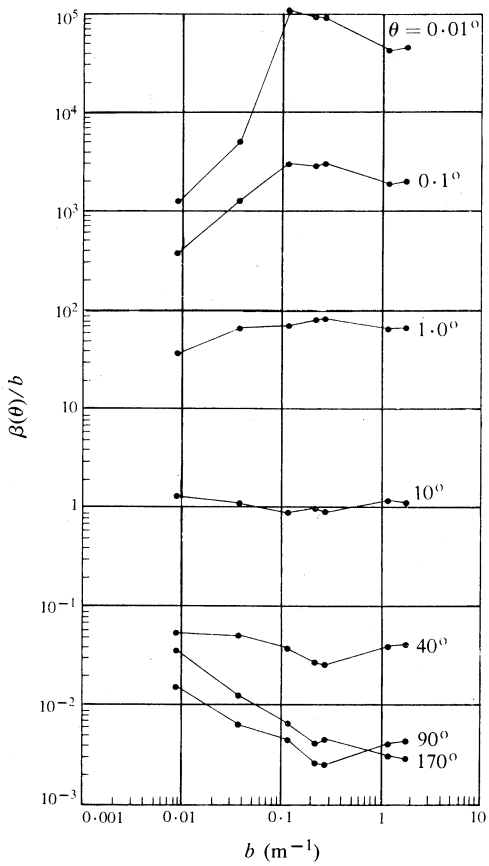

Fig. 6. Dependence of the normalized volume scattering function on the scattering coefficient (derived from Petzold's 1972 data).

For the volume scattering function $\beta(\theta)$, the experimental data obtained by Petzold (1972) were used. In the simulation program, basic $\beta(\theta)$ data were provided in the form of tables for seven representative curves measured at a wavelength of 530 nm in waters having a range of b values from 0·009 to 1·818 m^{-1}. During the operation of the program, appropriate data for $\beta(\theta)$ were generated for the particular values of b required in the simulation study by interpolation (or extrapolation) of the tabulated basic data. The accuracy of this operation was significantly improved by first normalizing the $\beta(\theta)$ data by dividing by the corresponding values of b to produce nearly constant-valued functions versus b for each of the tabulated values of the scattering angle θ (examples are shown in Fig. 6). The variation in $\beta(\theta)/b$

with b is due to different particle size distributions in waters of different turbidities (Jerlov 1976). Values of the cumulative probability

$$\Pi(\theta) = b^{-1} 2\pi \int_0^{\theta} \beta(\theta) \sin\theta \, d\theta \tag{18}$$

were then obtained by numerical integration.

Table 1. Assumed data of optical properties of water

Coefficient				
Attenuation c (m^{-1})	Absorption a (m^{-1})	Scattering b (m^{-1})	Backscattering b_b (m^{-1})	Single scattering albedo ω_0
0·1	0·0725	0·0275	0·0016	0·275
0·5	0·128	0·372	0·0057	0·744
2·0	0·337	1·663	0·033	0·832
5·0	0·754	4·246	0·085	0·849

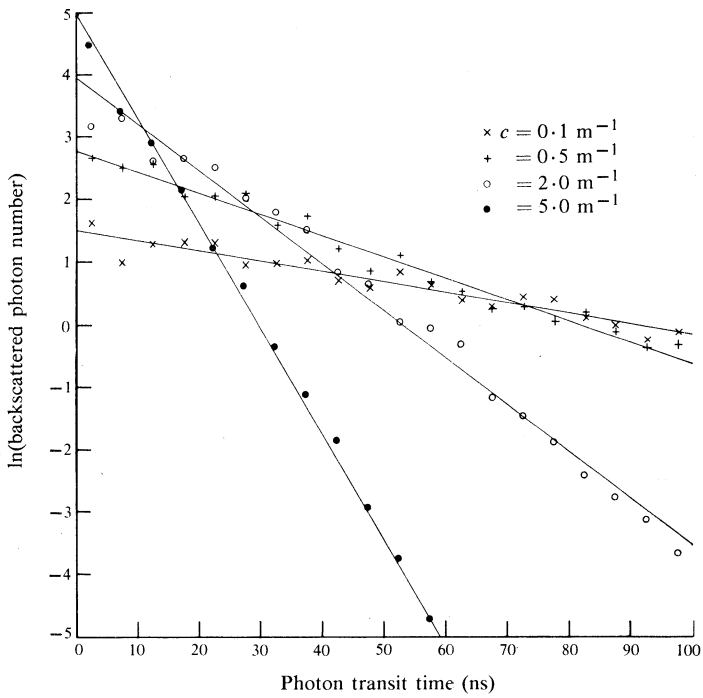

Fig. 7. Simulated decay with time of the backscattered photons reaching the airborne receiver (assuming 10^6 photons in the transmitted pulse, and 10 and 50 m radius at the sea surface and the receiver respectively.

The values of the backscattering coefficient b_b, corresponding to the selected values of c, were derived using the defining integral (14). These values, together with those for c, a and b and the single scattering albedo, are listed in Table 1.

(*c*) *Analysis of Computed Backscatter Signal*

The amplitude of the backscattered signal is expected to decay exponentially in accordance with equation (6), which may be rewritten, after taking logarithms, in the simplified form

$$\ln\{P'(t)\} = \ln\{B\beta(\pi)\} - 2kvt, \tag{19a}$$

where

$$B = (A/2h^2n^2)(1-\rho)^2vQ. \tag{19b}$$

The simulated backscatter signals from the full Monte Carlo model are presented in Fig. 7 together with corresponding lines of best fit calculated from the data using linear regression analysis.

The data shown in Fig. 7 are scaled to correspond to 10^6 transmitted photons in each pulse. In fact, the number of photon trajectories for each value of c was increased until the errors in the slope and intercept were reduced to acceptable values. The total numbers of photon trajectories computed were 16·8, 3·0, 0·6 and 0·6 million for $c = 0{\cdot}1$, $0{\cdot}5$, $2{\cdot}0$ and $5{\cdot}0\ \mathrm{m}^{-1}$ respectively. The results indicated that further increases in the numbers of photons traced would not reduce the errors significantly—presumably because the accuracy limit of the Monte Carlo model was being approached.

The slope of the regression line was used to obtain the effective attenuation coefficient k (with the aid of equation 19a). The validity of the inequality (16) could then be assessed using the values of a and b_b taken from Table 1.

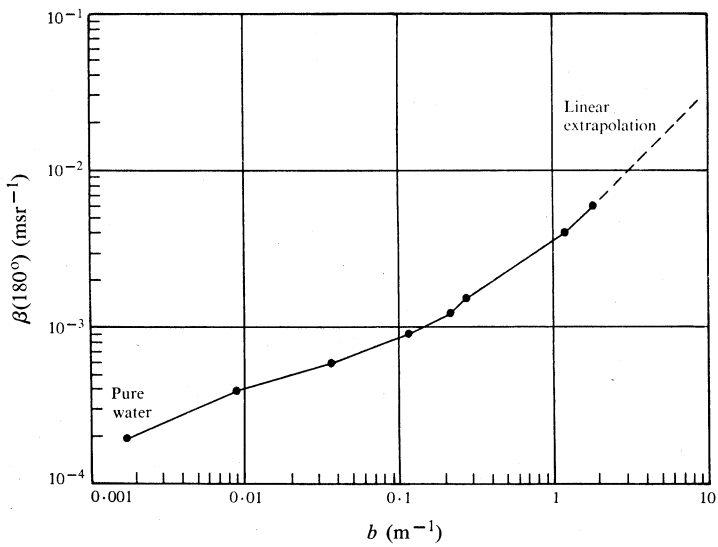

Fig. 8. Relationship between the volume scattering function at 180° (or π radians) and the scattering coefficient (derived from Petzold's 1972 data).

The intercept of the regression line was used to obtain an effective value of $\beta(\pi)$, again using equation (19a). The validity of the analytic model was tested by obtaining an effective value of the scattering coefficient b from the effective value of $\beta(\pi)$. The relationship between $\beta(\pi)$ and b used for this transformation was derived from the

data given by Petzold (1972) and is shown in Fig. 8. It can be seen that the relationship is nonlinear, particularly in relatively clear water. In turbid water the curve appears to approach a linear relationship and, consequently, a linear extrapolation is used for values beyond the last available data point. The standard errors in the slope and intercept were computed from the scatter of data points about the regression line. The corresponding errors in the derived values of k and b were then calculated.

The analysis was carried out on the data obtained for the six different receiver fields of view for which the Monte Carlo simulations were performed. For the two smallest fields of view, only photons collected in the inner receiver annuli were used, to avoid vignetting effects on the backscattered light produced at the greater depths.

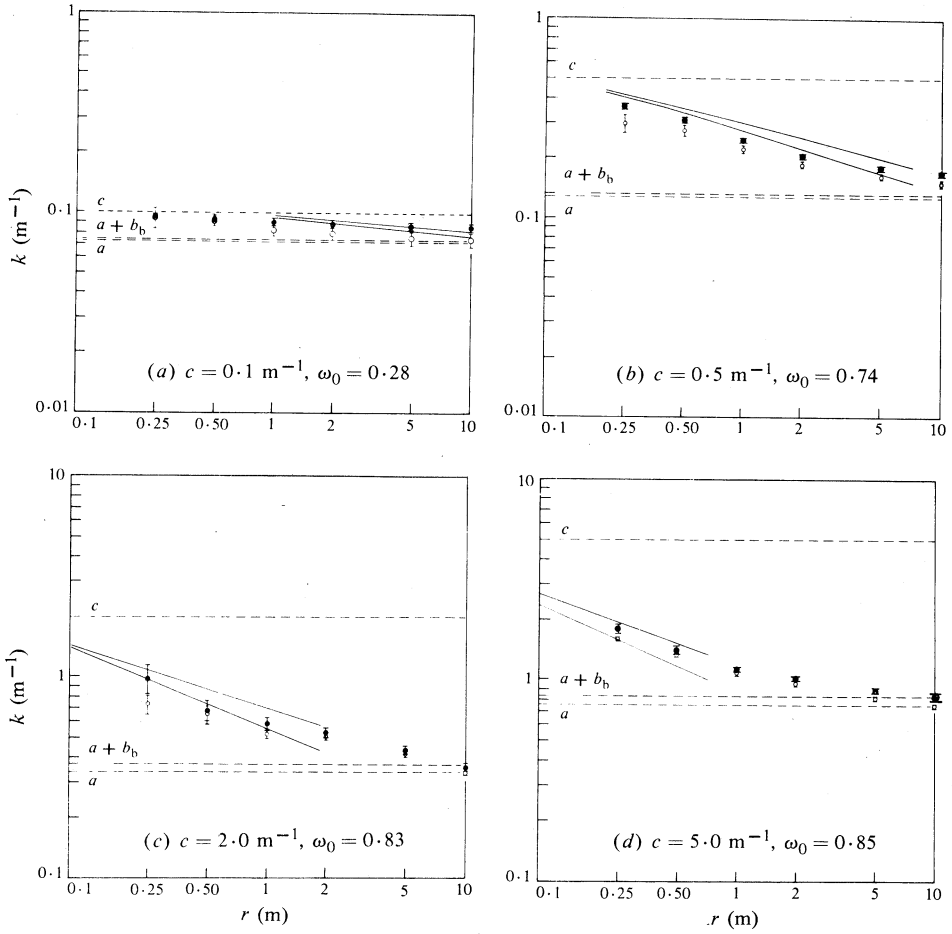

Fig. 9. Dependence of the effective attenuation coefficient k on the radius r of the receiver field at the sea surface for the four cases indicated. The aircraft height is assumed to be 500 m. Open and solid circles are for the full and semi-analytic Monte Carlo methods respectively.

(d) Results

Fig. 9 shows the dependence of the computed effective attenuation coefficient on the receiver field of view, which is represented by the radius of the field at the water surface when the aircraft height is 500 m. The open circles represent the values

obtained using the full Monte Carlo method, whereas the solid circles represent results of the semi-analytic Monte Carlo method. In both cases, the error bars indicate the standard errors determined from the regression analysis. The two solid lines in each part are the values derived by Gordon (1982) using two different volume scattering functions. Also shown for comparison are the values of a and $a+b_b$ (dashed lines), which are related by the inequality (16) to the minimum and maximum values of k expected in the large field of view limit. In addition, the expected value of k in the small single scattering albedo limit for a small field of view (namely c, see Section 2*e*) is shown.

It is evident from Fig. 9 that the coefficients obtained using the semi-analytic Monte Carlo method are consistent with the values obtained by Gordon (1982) using the same method. Both are consistently greater than those derived using the full Monte Carlo method. The differences, however, are only marginally significant.

The results show that, in all cases, the value of k decreases as the field of view increases. For the full Monte Carlo model, in all cases except $c = 0{\cdot}5\ \mathrm{m}^{-1}$ (see Fig. 9*b*), k has reached the asymptotic value a at a radius of 10 m. When $c = 0{\cdot}5\ \mathrm{m}^{-1}$ it appears that the value of k is still decreasing and requires a greater field of view to reach the asymptotic limit.

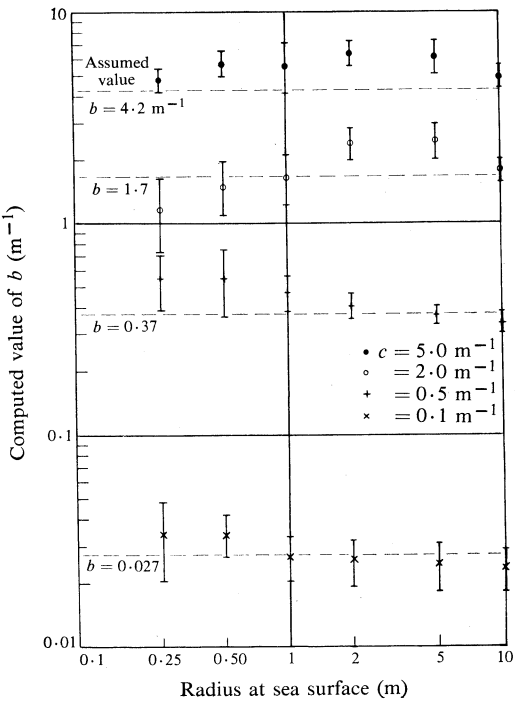

Fig. 10. Values of the scattering coefficient b computed for the four values of c indicated.

Only the two most turbid cases $c = 2{\cdot}0$ and $5{\cdot}0\ \mathrm{m}^{-1}$ (see Figs 9*c* and 9*d*) provide sufficient separation of the lower and upper limits of k, combined with small enough errors, to be able to distinguish them. The data from the full Monte Carlo model indicate that the asymptotic value of k is the absorption coefficient a, namely the lower limit in (16). Hence it would seem very little radiation is lost by backscattering.

The Monte Carlo simulation provides evidence of the validity of the analytic model in the large field of view limit over the full range of turbidities studied. The simulation does suggest, however, that the full field of view of 40 mrad (or a 10 m radius) available in the WRELADS system is marginal for determination of the absorption coefficient by this method and a larger field would be desirable for intermediate values of turbidity.

In the small field of view limit, the backscatter attenuation coefficient approached the value of c only in the low turbidity, low albedo case ($c = 0{\cdot}1\ \mathrm{m}^{-1}$ and $\omega_0 = 0{\cdot}28$; see Fig. 9*a*). In all other cases, the value of k lies significantly below the value of c at all fields of view studied.

The dependence of the computed values of the scattering coefficient b on the receiver field of view is shown in Fig. 10. For comparison the assumed values of b are also shown. It can be seen that in most cases the derived values are consistent with the assumed values. The errors are larger than for the values of k, partly because of the transformation from $\beta(\pi)$ to b (using Fig. 8) which increases errors.

The results show no significant dependence of the computed value of b on field of view. There is some evidence of the computed values of b being larger than the assumed value in the most turbid case ($b = 4{\cdot}2\ \mathrm{m}^{-1}$). This suggests that multiple scattering in very turbid water is beginning to produce a departure from the simple analytic model.

(*e*) *Discussion*

The small but consistent differences between the results obtained with the two Monte Carlo methods suggest that either or both methods need further refinement. When the field of view is large (e.g. $r = 10$ m) the full Monte Carlo model is preferred, because the large number of photons traced produces a small error and the method is not subject to the occasional 'spikes' observed with the semi-analytic model. However, at small fields of view, the semi-analytic model may be more accurate.

The results from the full Monte Carlo model show that the asymptotic limit of the effective attenuation coefficient k is the absorption coefficient a, rather than the diffuse attenuation coefficient K as stated by Gordon (1982). Actually, Gordon's Fig. 5 shows that the asymptotic value of k is less than K when $\omega_0 = 0{\cdot}3$ and $0{\cdot}5$. In the other cases ($\omega_0 = 0{\cdot}7$ and $0{\cdot}9$) the asymptotic values are not achieved at the largest field of view reported.

A possible explanation for k approaching a in the large field of view limit becomes evident when the independent variable in the model is considered to be time rather than depth. Every photon received at a given time has spent the same amount of time in the water and has also travelled the same total distance in the water, irrespective of how many times it has been scattered. Since the only process reducing the number of such photons is absorption, the effective attenuation coefficient equals the absorption coefficient.

4. Conclusions

The Monte Carlo simulation of laser backscatter from sea water shows that the analytic model is adequate over the range of beam attenuation coefficients studied, namely $0{\cdot}1$ to $5{\cdot}0\ \mathrm{m}^{-1}$. The value of the attenuation coefficient in the analytic model approximates the absorption coefficient of water a, only if the field of view

of the receiver is sufficiently large to observe a spot of at least 10 m radius on the water surface when the receiver is 500 m above the surface. Apart from the geometry of the receiving system the backscatter amplitude at the surface depends only on the scattering coefficient of the water.

This study shows, therefore, that it is possible in principle to determine both the absorption and scattering coefficients of water independently from an aircraft.

Acknowledgment

The authors wish to acknowledge the assistance provided by Mr W. Graveney in maintaining and operating the absorption meter and transmissometer equipment used for measurements of absorption and attenuation coefficients.

References

Austin, R. W., and Petzold, T. J. (1977). *In* 'Light in the Sea', Benchmark Papers in Optics, Vol. 3 (Ed. J. E. Tyler), pp. 104–20 (Dowden, Hutchinson and Ross: Stroudsburg).
Bauer, D., Brun-Cotton, C., and Saliot, A. (1971). *Cah. Oceanogr.* **23**, 841.
Calder, M. (1980). *Int. Hydrogr. Rev.* **52**, 31.
Clegg, J. E., and Penny, M. F. (1978). *Navigation* **31**, 52.
Gilbert, G. D., Honey, R. C., Myers, R. E., and Sorenson, G. P. (1969). Optical absorption meter. Final Report, April 1969, Stanford Research Institute Project No. 7440.
Gordon, H. R. (1982). *Appl. Opt.* **21**, 2996.
Hickman, G. D., and Hogg, J. E. (1969). *Remote Sensing Environ.* **1**, 47.
Hoge, F. E., Swift, R. N., and Frederick, E. B. (1980). *Appl. Opt.* **19**, 871.
Ivanov, A. P., Skrelin, A. L., and Sherbaf, I. D. (1972). *J. Appl. Spectrosc.* (*USSR*) **17**, 1087.
Jerlov, N. G. (1976). 'Marine Optics', Elsevier Oceanography Series, Vol. 14 (Elsevier Scientific: Amsterdam).
Kim, H. H. (1977). *Appl. Opt.* **16**, 46.
Penny, M. F. (1982). Proc. Int. Conf. on Lasers, New Orleans 14–18 Dec. 1981, p. 1029.
Petzold, T. J. (1972). Volume scattering functions for selected ocean waters. Final Report, Oct. 1972, Scripps Institution of Oceanography Ref. 72–8.
Phillips, D. M. (1979). *Aust. J. Phys.* **32**, 469.
Phillips, D. M., and Scholz, M. L. (1982). *Aust. J. Mar. Freshw. Res.* **33**, 723.
Plass, G. N., and Kattawar, G. W. (1971). *Appl. Opt.* **10**, 2304.
Platt, C. M. R. (1981). *J. Atmos. Sci.* **38**, 156.
Poole, L. R., Venable, D. D., and Campbell, J. W. (1981). *Appl. Opt.* **20**, 3653.
Preisendorfer, R. W. (1977). *In* 'Light in the Sea', Benchmark Papers in Optics, Vol. 3 (Ed. J. E. Tyler), pp. 46–64 (Dowden, Hutchinson and Ross: Stroudsburg).
Sizgoric, S., and Carswell, A. I. (1973). *Can. Aeronaut. Space J.* **19**, 511; M1.
Tyler, J. E. (Ed.) (1977). 'Light in the Sea', Benchmark Papers in Optics, Vol. 3 (Dowden, Hutchinson and Ross: Stroudsburg).

Manuscript received 9 June 1982, accepted 5 August 1983